

CHAPTER 125

Pressure Oscillations during Wave Impact on Vertical Walls

M.E.Topliss* M.J.Cooker[†] D.H.Peregrine[‡]

Introduction

This area of study concerns wave impact pressure on vertical structures. Severe damage can be inflicted on coastal defences during storms and numerous laboratory experiments have been undertaken to gain an understanding of the physical processes. This paper gives a mathematical description of high frequency pressure oscillations which are observed in measurements of water-wave impacts; particularly impact against a vertical wall. Our ultimate aim is to trace the physical origins of the pressure fluctuations which are related to the understanding of the role of fluid compressibility in breaking wave impact pressure. It has been suggested by some authors that the recorded pressure oscillations are due to the vibrations of air-filled gas bubbles, for example Weggel & Maxwell (1970) model some details of acoustic wave propagation. In addition, it is well known that the compressibility of a small volume fraction of air in water dramatically reduces the velocity of sound in the mixture. We investigate possible cases by simplifying the geometry and finding the frequency of free oscillations. We ignore the main flow of water since it has a longer time-scale. Our initial model considers compressible aerated water near the wall and compressible non-aerated water with a much higher sound speed further away. This is compared with a simple example of an air pocket trapped against a wall in incompressible water. Comparisons with three experimental results are encouraging.

*Research Student, School of Mathematics, Bristol University, Bristol BS8 1TW

[†]Research Assistant, School of Mathematics, Bristol University, Bristol BS8 1TW

[‡]Professor of Mathematics, School of Mathematics, Bristol University, Bristol BS8 1TW

Bubbly mixture near a wall

This model applies to the instances when a wave has broken creating a volume of water with many small bubbles next to the impact wall. This is now a compressible mixture.

Consider a region of uniform bubbly mixture (region 1) with a gas fraction α next to a vertical wall, and non-aerated water on the other side (region 2) as shown in figure 1.

We treat the solid wall and solid bed as rigid so that the component of displacement normal to these boundaries vanishes. As there is a large density contrast between the fluid and the air above, we take the pressure to vanish at the free surface. For linearised theory and sinusoidally varying velocity potential $\phi(x, y) e^{i\omega t}$ this implies ϕ may be taken to be zero on the free surface.

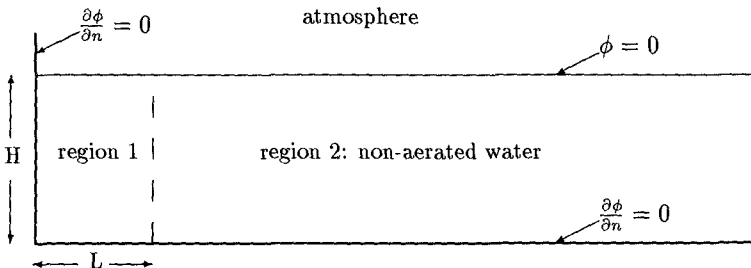


Figure 1. Limited volume of bubbly water

Sound waves are weak pressure disturbances which propagate at high speed through a fluid. The sound velocity in air is approximately 340 metres per second; that in water is approximately 1500 metres per second. In a mixture of air and water however, the speed of sound is dramatically reduced. The density in region 1 is taken to be $\rho_1 = (1 - \alpha)\rho_2$ where ρ_2 is the density in region 2. We have taken the speed of sound in region 1 as derived by Hsieh & Plesset (1961) to be

$$c_1^2 = \frac{\gamma p}{\rho_1 \alpha (1 - \alpha)},$$

where p is the atmospheric pressure, ρ_1 is defined above, γ is the ratio of specific heats, α is the gas fraction. For example 1 percent, 4 percent and 10 percent aeration give sound speeds of 120 m/s, 60 m/s and 40 m/s respectively, and this accords with experimental measures. The expression for c^2 is a good empirical rule provided α is not too near 0 or 1.

Viscosity and gravitational effects will be ignored. The reduced wave equation,

$$(\nabla^2 + k_i^2) \phi_i = 0$$

where the subscripts $i = 1, 2$ refers to regions 1, 2 respectively and $k_i = \omega/c_i$ where $\omega = 2\pi f$, is solved by separation of variables.

As the free surface and the rigid bed are totally reflecting surfaces the fluid can be considered as an acoustic plane waveguide and a standing wave field results, which has a cut-off frequency ω_n for each mode of oscillation, below which no propagation occurs. In region 2 the sound speed is very much higher and therefore ω may be less than the cut-off frequency and there is no propagation. The velocity potential for the bubbly mixture in this instance is:

$$\phi_1 = A_1 e^{\sqrt{k_1^2 - \gamma_n^2} L} \cos(\gamma_n y) \cosh \left[\sqrt{k_1^2 - \gamma_n^2} (x + L) \right] e^{i\omega t}$$

and for the non-aerated water outside the bubbly mixture is

$$\phi_2 = A_1 e^{\sqrt{k_1^2 - \gamma_n^2} L} (1 - \alpha) \cos(\gamma_n y) \cosh \left[\sqrt{k_1^2 - \gamma_n^2} L \right] e^{-\sqrt{\gamma_n^2 - k_2^2} x} e^{i\omega t}$$

where c_2 = the speed of sound in non-aerated water, $\gamma_n = n\pi/2H$, $n = 1, 3, 5, \dots$, H is the depth of the fluid, L is the width of the bubbly layer, A_1 is a constant.

Assuming pressure and normal velocity are continuous across the interface between region 1 and region 2, we find an expression for the frequency of modes of oscillations trapped in region 1:

$$(1 - \alpha) \sqrt{\gamma_n^2 - k_2^2} = \sqrt{k_1^2 - \gamma_n^2} \tan \left[\sqrt{k_1^2 - \gamma_n^2} L \right]$$

For a fixed width and air content, a high free surface will give a low frequency as illustrated in figure 2. Figure 3 shows that, for a fixed amount of air and depth, a wider region will have a lower frequency. Conversely a very narrow band of bubbles against a rigid wall will produce very high frequencies. Both figures show higher frequencies with a lower aeration level.

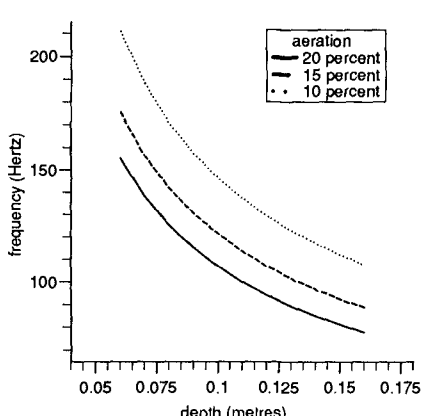


Figure 2. Variation of f with H

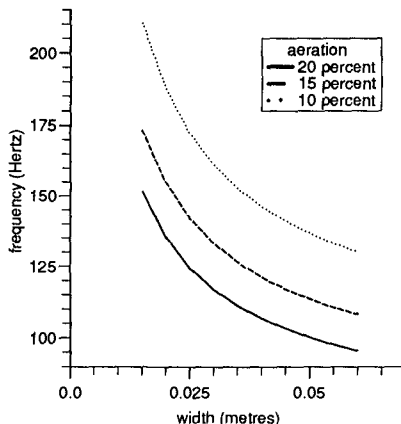


Figure 3. Variation of f with L

A trapped air pocket

To model of a trapped air pocket against a vertical wall we now have to take into account a) the presence of the free surface, b) the cylindrical geometry of the gas pocket, c) the presence of the rigid wall.

Suppose the bubble contains air at atmospheric pressure and that it's centre is submerged a distance h below the free surface and lies a distance d above the seabed as shown in figure 4. The water is taken to be incompressible.

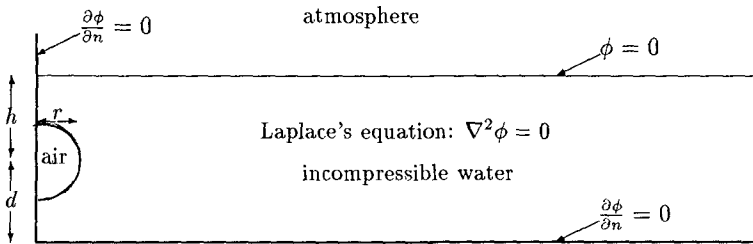


Figure 4. Trapped air pocket at the wall

We model the vibrations of the trapped air pocket by considering the radial oscillations, translation and shape oscillations of a single two dimensional bubble with semi-circular cross-section of radius r . As this study concerns only relatively large bubbles, surface tension effects can be neglected as they are only significant for small radii. During the short time in which the bubble oscillates regularly we suppose that the free surface moves very little so that we may again ignore the flow in the impacting wave. We take an image of the bubble above the free surface to be oscillating in anti-phase with respect to the bubble, an image below the rigid bed to be oscillating in phase, and a third image below, oscillating in anti-phase, to ensure symmetry as shown in figure 5. These images then extend above and below to produce an infinite series which is summed analytically. The potential for this model is

$$\phi = -\alpha_0 \log \left[\frac{\cosh(\lambda z) - \cos(\lambda d)}{\cosh(\lambda z) + \cos(\lambda d)} \right] + \frac{\alpha_1}{(z - z_0)} + \frac{\alpha_2}{(z - z_0)^2}$$

where $\lambda = \pi/2(d + h)$, z_0 = the position of the bubble, $i = \sqrt{-1}$, $\alpha_0, \alpha_1, \alpha_2$ are constants. Figure 6 shows the pressure contours from a two dimensional bubble.

The logarithmic term, which is the dominant term, represents the radial oscillations. The second term, evaluated on the bubble surface,

$$\frac{\alpha_1}{(z - z_0)} = -\alpha_0 \frac{\lambda r}{2} [\cot \lambda d + \tan \lambda d] \sin \theta,$$

represents translational motion and the third term, evaluated on the bubble

surface,

$$\frac{\alpha_2}{(z - z_0)^2} = \alpha_0 \frac{\lambda^2 r^2}{8} [4 + \tan^2 \lambda d - \cot^2 \lambda d] (2 \cos^2 \theta - 1),$$

represents a first approximation to shape oscillations.

We calculate the time-harmonic irrotational flow induced by the semicircular two dimensional bubble and the frequency of the small oscillations is given by

$$\omega^2 = -\frac{2\gamma p [1 + \frac{1}{2}\lambda^2 r^2]}{\rho r^2 [\log(\frac{1}{2}\lambda r \tan \lambda d) + \frac{1}{4}\lambda^2 r^2]}$$

p is the atmospheric pressure, ρ is the density of water. As figure 7 shows, for fixed $h + d$, an air pocket nearer the rigid bed will have a lower resonant frequency than an air pocket nearer the free surface. The size of the air pocket is inversely proportional to the frequency as illustrated in figure 8. This corresponds to the previous model for the bubbly mixture which showed high frequencies are obtained for lower aeration.

i) as h becomes large,

$$\omega^2 = -\frac{2\gamma p}{\rho r^2 \log [2rd/R]},$$

the frequency for a single two dimensional bubble in the vicinity of a rigid boundary, where R is a large number representing a boundary far away. This is to ensure boundary conditions in the far field are satisfied.

ii) as d becomes large,

$$\omega^2 = -\frac{2\gamma p}{\rho r^2 \log [r/2h]},$$

the frequency for a single two dimensional bubble in the vicinity of a free boundary (Topliss 1991).

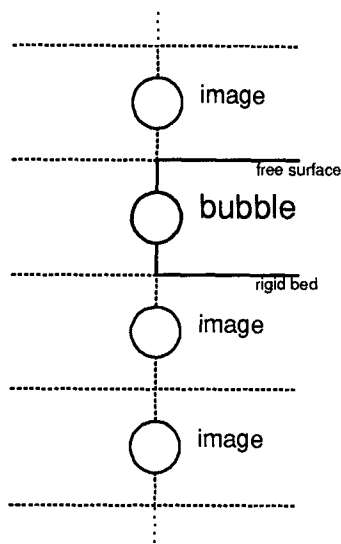


Figure 5. Bubble and three images

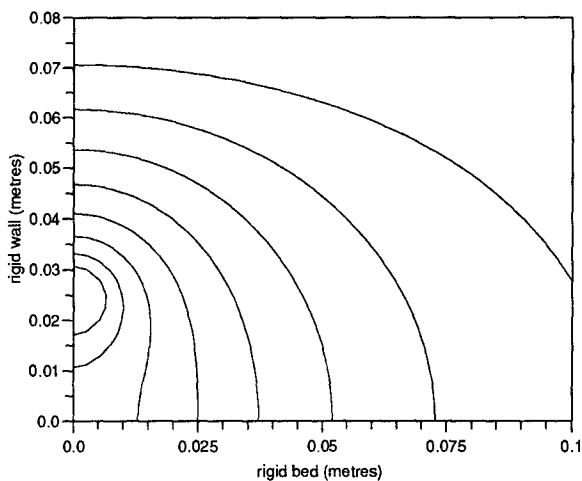


Figure 6. Pressure contours from single bubble on wall

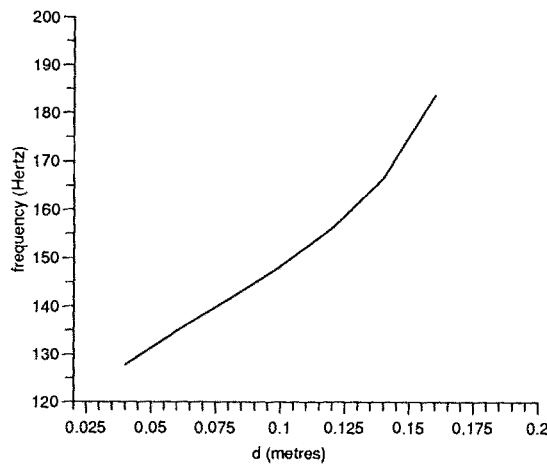


Figure 7. Variation of frequency with d

$h+d$ fixed at 0.2 m, $r=0.01$ m

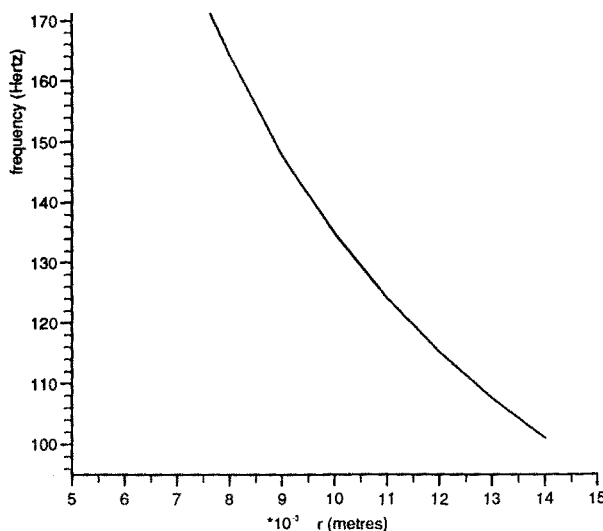


Figure 8. Variation of frequency with radius

$h+d$ fixed at 0.2 m, $h=0.14$ m, $d=0.06$ m

Comparisons with experiments

We have considered three experimental studies for comparison with these theoretical results:

I) Hattori & Arami (1992); Chuo University, Japan

Hattori & Arami have provided us with many details of their experiments which investigate the importance of an air pocket between the breaking wave and the wall. The experiments were undertaken in a small wave tank (still water depth at the wall of five centimetres) and high-speed video frames were taken of waves as they impact on a vertical wall and some waves appear to trap a cylinder of air against the wall. Records from six pressure gauges of one centimetre diameter are available.

The histories of the pressure, measured at the wall, for these waves exhibit three stages. Initially the pressure rises to a peak value and is followed by an interval of regular smooth oscillations, of decreasing amplitude. These oscillations are displayed with the same frequency in all six pressure gauges. Clearly this decay requires further modelling. This finally develops into a more confused signal, consisting of higher frequencies with lower amplitudes, and which carries on for an indefinite time.

As the wave advances towards the impact structure, it begins to curl over, entrapping an air pocket against the wall. In the video frames following the impact, it can be seen that the free surface rises and a thin jet of water shoots up the wall. We neglect this since it is usually much thinner than the bubble until a later stage and assume a flat surface in our models. For each experiment we have considered, we have taken measurements from the first three frames at the beginning of the oscillations and compared the frequency calculated for that geometry with the frequency given by the pressure gauges. The theory compares particularly well for large air pockets, see table 1.

II) Witte (1988); Leichtweiss-Institut, Germany

Witte describes a wave impact against a vertical wall and observed an air pocket trapped against the impact wall. The wave tank had a still water depth at the wall of sixteen centimetres and fourteen pressure cells. Full details are given of one case (example no.13, figure 6.3, type II). Regular oscillations are recorded in all cells of period 12 milliseconds, or a frequency of 83.3 Hertz. If we choose $h = 0.22$ m and $d = 0.05$ m (no photographs are given but the description given by Witte suggests that the air pocket is nearer the bed than the free surface) then, from figure 9 below where the variation of frequency with size of air pocket is presented, a bubble of radius 0.0155 m would give a frequency of 83 Hertz. Although no photos are available, the statistics presented in Witte (1988) for this type of impact give scope for further study.

description				Topliss	Hattori
	distance d (metres)	distance h (metres)	radius r (metres)	frequency f (Hertz)	frequency f (Hertz)
data No.1-031-3					
frame 715	0.06	0.016	0.011	235	210
frame 720	0.06	0.017	0.011	228	210
frame 725	0.061	0.017	0.011	228	210
data No.172-3					
frame 815	0.031	0.038	0.007	233	210
frame 820	0.032	0.04	0.007	231	210
frame 825	0.033	0.042	0.007	229	210
data No.132-3					
frame 295	0.031	0.024	0.008	241	190
frame 300	0.031	0.04	0.008	207	190
frame 305	0.031	0.044	0.008	202	190
data No.178-3					
frame 320	0.027	0.025	0.02	142	104
frame 325	0.029	0.041	0.02	106	104
frame 330	0.029	0.043	0.02	104	104
data No.152-6					
frame 015	0.029	0.044	0.024	93	100
frame 020	0.03	0.047	0.024	90	100
frame 025	0.03	0.05	0.024	87	100
data No.2-255-4					
frame 330	0.032	0.037	0.02	113	99
frame 335	0.032	0.044	0.02	104	99
frame 340	0.032	0.049	0.02	99	99

Table 1. Comparison of experimental data and theory. The frames are separated by a timestep of five milliseconds and $f = \omega/2\pi$

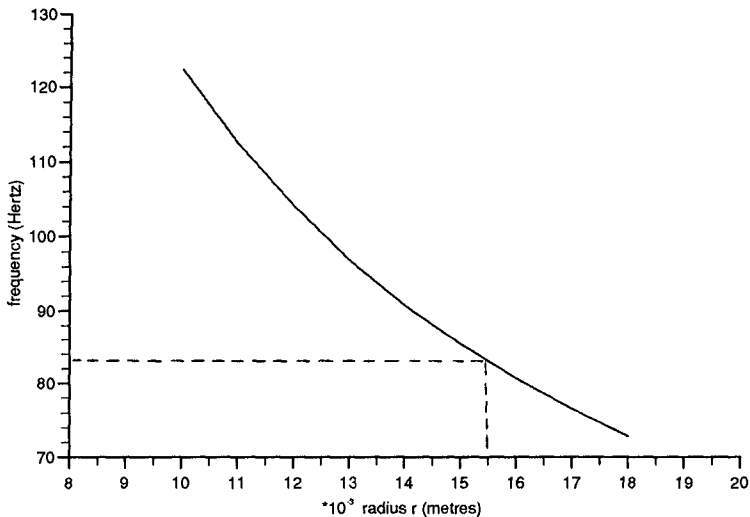


Figure 9. Comparison of theory with data

$$h = 0.22 \text{ m}, d = 0.05 \text{ m}$$

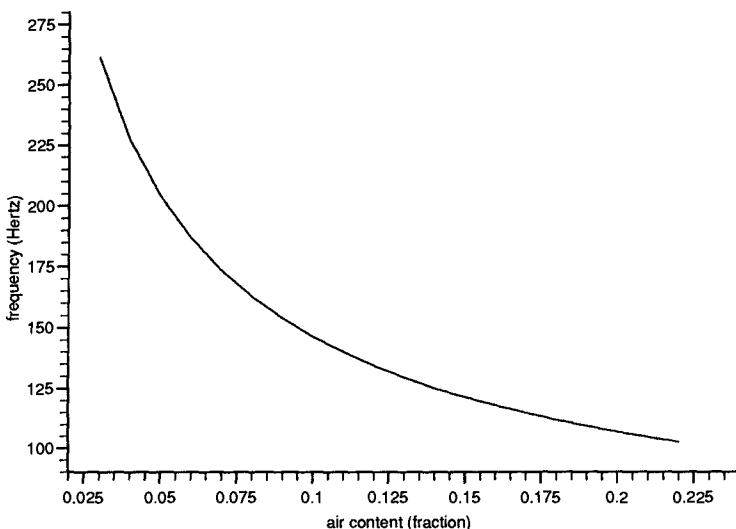


Figure 10. Comparison of theory with data

III) Graham & Hewson (1992); Plymouth University, England

Graham & Hewson have carried out model-scale experiments of waves breaking against a vertical wall, with three pressure transducers and one aeration gauge in order to investigate aeration levels of a wave impacting upon structures. No previous work (to our knowledge) has been carried out on aeration measurements and with the kind permission of Graham & Hewson we are able to compare our theoretical work with the preliminary work carried out at Plymouth. Video frames are not yet available.

After impact the pressure transducers show both rapid fluctuations and an underlying frequency of approximately 30-40 Hertz. Although we have been unable to find an example which would give a frequency this low, the rapid fluctuations are in the range of 100-300 Hertz which is consistent with other experiments. The levels of aeration shown range between 4 percent and 20 percent. If we estimate the depth of the water at the wall to be 0.1 metres and the width of the bubbles to be 0.04 metres we can expect frequencies of between 100 and 260 Hertz, as illustrated in figure 10. These are within the range of frequencies measured in the experiments.

Discussion

We have not yet been able to compare the theory with large scale experiments, although studies are been undertaken in Hannover (Schmidt, Oumeraci & Partenscky 1992), where double peak forces have been recorded along with negative pressures. Table 2 gives examples of how scale effects could vary the frequencies according to the size and position of an air pocket trapped. We have taken an example from table 1 (data No.132-3) and altered the geometric parameters.

	radius r (metres)	distance d (metres)	distance h (metres)	frequency f (Hertz)
	0.008	0.031	0.040	207
x 5	0.04	0.155	0.2	42
x 10	0.08	0.31	0.4	21
x 50	0.4	1.55	2.0	4.2
x 100	0.8	3.1	4.0	2.1

Table 2. Variation of geometries for a trapped air pocket

For a wave which breaks giving a bubbly mixture, table 3 gives examples of frequencies which could be obtained in a larger volume. Here we have taken the gas fraction to be 0.1.

	height H (metres)	width L (metres)	frequency f (Hertz)
	0.1	0.04	146
x 5	0.5	0.2	106
x 10	1.0	0.4	14.6
x 50	5.0	2.0	10.6
x 100	10.0	4.0	1.46

Table 3. Variation of geometries for a bubbly mixture

Table 2 and 3 show that the frequency varies linearly with the geometric parameters, a property easily deduced from the equations. For the lowest frequency shown above, a typical compressible length = wavelength / 2π which is approximately 160 metres in pure water but only 5 metres for 10 percent aeration indicates that for the largest waves that trap air, sound propagation is important as has been noted by Schmidt, Oumeraci & Partenscky.

This work has only studied free oscillations. The initial forcing, amplitude and damping of the oscillations all require further study. The decay of the regular oscillations, well illustrated by the experiments of Hattori & Arami (1992), are due to damping which could be the result of several mechanisms: viscous damping, thermal damping or acoustic radiation. There are also radiating modes which need investigation.

The financial assistance of SERC is gratefully acknowledged.

References

- GRAHAM,D.I & HEWSON,P.J: (1992) Measurement of aeration in model-scale breaking waves. *Mast G6-S/Project 2*, Informal Internal Report.
- HATTORI,M & ARAMI,A: (1992) Impact breaking wave pressures on vertical wall. *23rd Int. Coastal Engineering Conf.*, Venice, Italy.
- HSEIH,D.Y & PLESSET,M.S: (1961) Theory of rectified diffusion of mass into gas bubbles. *J.Acoust.Soc.Am* **33** no. 2
- SCHMIDT,R., OUMERACI,H & PARTENSCKY,H.-W: (1992) Impact Loads Induced by Plunging Breakers on Vertical Structures. *23rd Int. Coastal Engineering Conf.*, Venice, Italy.
- TOPLISS,M.E: (1991) *Mathematical description of air bubbles in water*. M.Sc Thesis, Bristol University.
- WEGGEL,J.R & MAXWELL,W.H.C: (1970) Numerical Model for wave pressure distributions. *J.Waterways, Harbors & Coastal Engineering Div*, Proc. ASCE **96** pp 623-642.
- WITTE,H.-H : (1988) Wave-induced impact loading in deterministic and stochastic reflection. *Mitteilungen*, Leichtweiss Institut fur Wasserbau, Tech. University Braunschweig, **102** pp ix-227.